Research Square

Preprints are preliminary reports that have not undergone peer review.
They should not be considered conclusive, used to inform clinical practice,
or referenced by the media as validated information.

RhoA G17E/Vav1 signaling induces cancer invasion via matrix metalloproteinase-9 in gastric cancer

Satoshi Nakamura
Shinshu University School of Medicine
Masato Kitazawa (kita118@shinshu-u.ac.jp)
Shinshu University School of Medicine
Yusuke Miyagawa
Shinshu University School of Medicine
Makoto Koyama
Shinshu University School of Medicine
Satoru Miyazaki
Shinshu University School of Medicine
Nao Hondo
Shinshu University School of Medicine
Futoshi Muranaka
Shinshu University School of Medicine
Shigeo Tokumaru
Shinshu University School of Medicine
Yuta Yamamoto
Shinshu University School of Medicine
Takehito Ehara
Shinshu University School of Medicine
Masatsugu Kuroiwa
Shinshu University School of Medicine
Hirokazu Tanaka
Shinshu University School of Medicine
Tomio Matsumura
Shinshu University School of Medicine
Michiko Takeoka
Shinshu University School of Medicine
Yuji Soejima
Shinshu University School of Medicine

Research Article

Keywords: Diffuse gastric cancer, RhoA, Vav1, Matrix metalloproteinase-9, Malignant phenotype

Posted Date: May 11th, 2021

DOI: https://doi.org/10.21203/rs.3.rs-434325/v1

License: This work is licensed under a Creative Commons Attribution 4.0 International License.
Read Full License

Abstract

Background: Ras homolog family member A (RhoA), a member of the Rho family of small GTPases, and Vav1, a guanine nucleotide exchange factor for Rho family GTPases, have been reported to activate pathways related to the actin cytoskeleton and regulation of cell shape, attachment, and motility. The interaction between these molecules in lymphoma is involved in malignant signaling, but its function in epithelial malignancy is unknown. Here, we investigated the malignant signal of mutant RhoA in gastric cancer and demonstrated the potential of RhoA G17E/Vav1 as a therapeutic target for diffuse gastric cancer.

Methods: The RhoA mutants R5W, G17E, and Y42C were retrovirally transduced into the gastric cancer cell line MKN74. The stably transduced cells were used for morphology, proliferation, and migration/invasion assays in vitro. MKN74 cells stably transduced with ectopic wild-type RhoA and mutant RhoA (G17E) were used in a peritoneal xenograft assay.

Results: The RhoA mutations G17E and Y42C induced morphological changes in MKN74. G17E induced Vav1 expression at the mRNA and protein levels and promoted the migration and invasion of MKN74. An RNA interference assay of Vav1 revealed that RhoA G17E enhanced cancer cell invasion via Vav1. Furthermore, immunoprecipitation revealed that Vav1 and RhoA G17E specifically bind and function together through matrix metalloproteinase-9. In a peritoneal xenograft model of nude mice, RhoA G17E promoted peritoneal dissemination, whereas Vav1 knockdown suppressed it.

Conclusion: Overall, our findings indicate that RhoA G17E associated with Vav1 and promoted cancer invasion via matrix metalloproteinase-9 in gastric cancer cells. Thus, RhoA G17E/Vav1 signaling in diffuse gastric cancer may be a useful therapeutic target.

Background

Gastric cancer remains the leading cause of cancer death worldwide [1, 2] and has two major histologic types: intestinal type and diffuse type [3]. The diffuse type, which exhibits sparse tumor cell infiltration into the gastric wall, has a worse prognosis [4] and has been described as a hereditary gastric cancer caused by CDH1 gene mutation [5]. Recent studies involving whole-exome or whole-genome sequencing revealed a RhoA mutation in 14.3–25.3% of diffuse type gastric cancers but not in intestinal type gastric cancers [6-8]. RhoA is a member of the family of small GTPases, which regulate cell migration, adhesion, proliferation, and differentiation [9]. RhoA activity has been reported to correlate with worse overall survival in diffuse gastric cancer. In vitro examination showed that RhoA mutations maintained cell survival by suppressing actin stress fiber formation in gastric cancer cells [10]. However, the effect of RhoA mutation on gastric cancer and its mechanism of action are not well-understood.

In this study, we focused on the Vav1-mediated malignant signal associated with RhoA mutation. Vav1 is member of the Dbl family of proteins, which function as guanine nucleotide exchange factors, activate Rho family small GTPases [11], and play key roles in the progression of human cancer [12-15].

Histologically positive expression of Vav1 was previously found to be correlated with a larger tumor size, greater lymph node metastasis, and serosal invasion; therefore, Vav1 expression was identified as an independent prognostic factor in patients with gastric cancer [16].

Here, we investigated the malignant phenotype resulting from RhoA mutations in gastric cancer. We found that RhoA G17E/Vav1 enhanced cancer invasion through matrix metalloproteinase-9 (MMP-9). Furthermore, we found that RhoA G17E induced Vav1 expression and was strongly involved in peritoneal dissemination.

Methods

Cell culture

The human gastric cancer cell line MKN74 was obtained from the Japanese Collection of Research Bioresources cell bank (JCRB Cell Bank, Osaka, Japan) and maintained in RPMI 1640 medium (Gibco, Grand Island, NY, USA). MKN74 is a moderately differentiated adenocarcinoma cell line possessing wild-type RhoA as well as other wild type mitogen-activated protein kinase (MAPK)-related molecules, such as EGFR, FGFR2, HER2, KRAS, NRAS, and BRAF. MKN74 cells were cultured in medium supplemented with 10% fetal bovine serum (Biowest, Nuaillé, France) and 1% penicillin/streptomycin at 37°C, in a 5% CO_2 atmosphere. Cell viability and counts were evaluated with a TC20™ Automated Cell Counter (Bio-Rad Laboratories, Hercules, CA) following trypan blue staining.

Antibodies and reagents

The following antibodies were used for western blotting: monoclonal mouse anti-phospho-Vav (sc-135788) from Santa Cruz Biotechnology (Dallas, TX, USA); monoclonal rabbit anti-Vav (#4657), monoclonal rabbit anti-RhoA (#2117), monoclonal rabbit anti-ROCK1 (#4035), monoclonal rabbit anti-cofilin (#5175), monoclonal rabbit anti-phospho-cofilin (#3313), polyclonal rabbit anti-SEK/MKK4 (#9152), monoclonal rabbit anti-phosphor-SEK (#4514), monoclonal rabbit anti-p38MAPK (#4511), and polyclonal rabbit anti-phosphor-p38MAPK (#9211) from Cell Signaling Technology (Danvers, MA, USA); and the secondary antibodies peroxidase conjugated anti-GAPDH (#015-25473) from FUJIFILM Wako Pure Chemical Corporation (Osaka, Japan); and goat anti mouse IgG/horseradish peroxidase (HRP; #P0447) and goat anti-rabbit IgG/HRP (#M7106) from DAKO (Santa Clara, CA, USA). ROCK inhibitor (Y-27632) was purchased from Selleck Chemicals (Houston, TX, USA).

Vector construction and retroviral transduction

The RhoA mutants R5W, G17E, and Y42C, with or without N-terminal FLAG, were created using the InFusion® HD Cloning Kit (Takara Bio, Shiga, Japan). The DNA sequences of all these mutants were confirmed by sequencing using the BigDye® Terminator v3.1 Cycle Sequencing Kit (Life Technologies, Carlsbad, CA, USA). The wild-type RhoA gene and RhoA mutants were inserted into the retroviral vector pDon5 Neo DNA (Takara Bio). For retroviral transduction, these vectors and an empty vector (Mock), as a

control, were transfected into the Phoenix packaging cell line using PEI MAX (Polysciences, Warrington, PA, USA). The virus-containing supernatants were collected after 24, 48, and 72 h, and the MKN74 cells were infected with the retrovirus particles on RetroNectin®-coated plates (Takara Bio). Stably transfected cells were obtained after G418 (Roche, Basel, Switzerland) selection for 10 days.

Reverse transcription-quantitative PCR

Total mRNA from MKN74 cells was extracted using NucleoSpin RNAplus (Takara Bio), and cDNA was synthesized using PrimeScript RT Master Mix (TaKaRa Bio) by incubation at 37°C for 15 min and 85°C for 5 sec. Quantitative PCR was conducted using SYBER Premix Ex Taq™ II (Takara Bio) and a Mastercycler realplex2 (Eppendorf, Hamburg, Germany). The thermocycling conditions were as follows: denaturation at 95°C for 2 min, followed by 40 cycles of 95°C for 15 sec, °C for 15 sec, and 68°C for 20 sec. Relative expression level was calculated using the $2^{-\Delta\Delta Cq}$ method [17]. All data were normalized to the expression level of GAPDH mRNA and were presented as the fold-increase in expression relative to that in the control cells. The following primers were used: RhoA forward, 5'-GTGTTTTTCCATCGACAGCC-3' and reverse, 5'-GCCTTGTGTGCTCATCATTC-3'; Vav1 forward, 5'-GCCTATGCAGCGAGTTCTCAA-3' and reverse, 5'-TTGTCTCGCTTGACCTCGTTC-3'; E-cadherin forward, 5'-AACAAGCCCGAATTCACCCA-3' and reverse, 5'- GCGGCATTGTAGGTGTTCAC-3'; Snail forward, 5'-ATCGGAAGCCTAACTACAGCG-3' and reverse, 5'- TCCCAGATGAGCATTGGCAG-3'; Slug forward, 5'- ACATTAGAACTCACACGGGGG-3' and reverse, 5'-AGAATGGGTCTGCAGATGAGC-3'; ZEB1 forward, 5'- ACCACCCTTGAAAGTGATCCA-3' and reverse, 5'-GCATTTTCTTTTTGGGCGGTG-3'; Vimentin forward, 5'- CACTCCCTCTGGTTGATACCC-3' and reverse, 5'-CGTGATGCTGAGAAGTTTCGT-3'; GAPDH forward, 5'-CACCACCAACTGCTTAGCACC-3' and reverse, 5'-CAGTCTTCTGGGTGGCAGTGATG-3'.

Western blot analysis

Cells were lysed in RIPA lysis buffer (sc-24948, Santa Cruz Biotechnology) containing phenylmethylsulfonyl fluoride, protease inhibitor cocktail, and sodium orthovanadate on ice for 30 min. The isolated protein was quantified using a Pierce BCA Protein Assay kit (Thermo Fisher Scientific, Waltham, MA, USA) and was then subjected to SDS-PAGE with NuPAGE® Bis-Tris Precast Gel (Invitrogen, Carlsbad, CA, USA) and transferred to a polyvinylidene fluoride membrane. Membranes were incubated with primary antibodies at 4°C overnight and then with HRP-conjugated secondary antibodies. Chemiluminescence was detected using the Amersham ECL Prime Western Blotting Detection Reagent (GE Healthcare, Buckinghamshire, UK). Blot imaging and analysis were performed using the ChemiDoc XRS+ System (Bio-Rad Laboratories).

Migration assay and invasion assay

Cells were dissociated with trypsin (Gibco) to form a single cell suspension using a 40-μm Corning® Cell Strainer (Corning, Inc., Corning, NY, USA) and counted with a TC20™ Automated Cell Counter (Bio-Rad Laboratories). Migration assays were performed using Falcon® Cell Culture Inserts and Companion Plates in a 24-well plate with an 8.0-μm Transparent PET Membrane (Falcon, Corning, Inc.). Cells ($5 \times 10^{5)}$

were suspended in 500 µL of serum-free medium and seeded into the upper chamber with or without 10 µM Y-27632 (Selleck Chemicals). The lower chamber was filled with medium containing 20% fetal bovine serum. After incubation for 24 h at 37℃, in an atmosphere containing 5% CO_2, migrated cells were fixed in 100% methanol for 10 min and stained with Giemsa Stain Solution (FUJIFILM Wako) for 30 min. The migrated cells were counted in five random fields per sample under a microscope at 200× magnification (Olympus Corporation, Tokyo, Japan). Invasion assays were performed using the same method as that used for the migration assays, with the following exceptions: 1×10^5 cells were seeded into the upper chamber of a Matrigel-coated transwell chamber (Corning® BioCoat™ Matrigel® Invasion Chambers 24 Well, Corning, Inc.), and invaded cells were counted after incubation for 48 h.

Knockdown of Vav1 using short hairpin RNA (shRNA) and small interfering RNA (siRNA)

The Vav1 knockdown vector was constructed using the pSINsi-hU6 shRNA expression retrovirus vector (Takara Bio) modified to be hygromycin B resistant. The target sequences for Vav1 shRNA and scramble shRNA (as a negative control) were as follows: Vav1 shRNA: 5'-CGTCGAGGTCAAGCACATT-3', scramble shRNA: 5'-TAAGCAGCGACGTATCGTC-3' (14,15). Stably transduced cells were selected using hygromycin B (FUJIFILM Wako) for 10 days. MISSION® siRNA(#NM_005428) and MISSION® siRNA Universal Negative Control #1 (SIC001) from Sigma-Aldrich (St. Louis, MO, USA) were transfected using Lipofectamine RNAi MAX Reagent (Thermo Fisher Scientific).

Immunoprecipitation

Lysates prepared using NP-40 lysis buffer (50 mM Tris-HCl, pH 7.5, 150 mM NaCl, 0.05% NP-40, Protease/Phosphatase Inhibitor Cocktail (#5879, Cell Signaling Technology) were incubated with Anti-DDDDK-tag pAb-Agarose (PM020-8, MBL, Nagoya, Japan) for 2 h at 4°C. After centrifugation, the beads were washed with NP-40 lysis buffer and then heated to 95°C for 5 min in sample buffer (FUJIFILM Wako). Following a brief centrifugation, the supernatants were separated by SDS-PAGE, and the protein detection was performed by immunoblotting.

Gelatin zymography

The cell culture supernatant was collected after 48 h of culture in serum-free medium. The supernatant was concentrated using Vivaspin® Turbo 15 (Sartorius Stedim Biotech GmbH, Goettingen, Germany). FITC-labeled precast gelatin gels and buffers for gelatin zymography were used in combination with the FITC-labeled Gelatin-zymography Kit (Cosmo Bio, Tokyo, Japan), according to the manufacturer's instructions. Briefly, the samples (2.5 µg) on gel-plates were electrophoresed at a constant current of 15 mA; the gels were then rinsed with wash buffer for 1 h. The enzyme reaction was performed by incubating the gels with an enzyme reaction buffer at 37°C for 24 h. The zymogram was imaged using the ChemiDoc XRS + system (Bio-Rad Laboratories) at an excitation wavelength of 535 mm.

Peritoneal xenograft model

Eight-week-old male BALB/c nu/nu mice were obtained from CLEA Japan (Tokyo, Japan). Cells (2×10^6) were resuspended in 200 µL of Hank's balanced salt solution (FUJIFILM Wako) and injected into the abdominal cavity of the mice. We used a breeding room in the Division of Animal Research, Shinshu University. The rearing environment was controlled at a room temperature of 22-25°C and humidity of 40-45%. Two mice were housed in one sufficiently large cage. At 4 weeks after transplantation, the mice were sacrificed by cervical dislocation under 3% isoflurane anesthesia, and the number of disseminated nodules in the abdominal cavity was counted. All animal experiments were performed according to the national standard of the care and use of laboratory animals, and the study was approved by the Institutional Animal Care and Use Committee with Shinshu University School of Medicine.

Statistical analysis

All statistical analyses were performed using the JMP software (SAS Institute, Cary, NC, USA). Statistical significance of differences was evaluated by Student’s t-test, Tukey's test, and Dunnett's test. Continuous variables were expressed as mean ± standard deviation. A P value <0.05 was considered to indicate a statistically significant result.

Results

RhoA mutation induced morphological changes but did not affect proliferation in well-differentiated gastric cancer cells

RhoA mutations in diffuse type gastric cancer have been reported to be frequent at codons 5, 17, 42, and 57 [6, 7]. The RhoA mutants R5W, G17E, Y42C and empty vector (Mock) were introduced retrovirally into the wild-type RhoA-containing gastric cancer cell line MKN74. Real-time PCR showed that the expression of RhoA mRNA was significantly increased by gene transfer; both transgenic RhoA and endogenous RhoA could be detected, indicating that gene transfer was successful (Fig. 1A). Similarly, RhoA protein expression was slightly increased in cells subjected to ectopic gene transduction (Fig. 1B). After constitutive transduction, morphological changes, including the formation of a spindle-shape and sharp edges, were clearly observed in G17E and weakly observed in Y42C (Fig. 1C); contrarily, a round shape and smooth edges were observed in wild-type RhoA-containing cells. We predicted that the RhoA mutants would alter cell proliferation; however, the cell counting assay (Fig. 1D) and CCK8 assay (data not shown) revealed no significant change in proliferation.

RhoA G17E promoted cancer migration and invasion in vitro

Next, migration and invasion assays were performed using the transwell system. In the migration assays, significantly more RhoA G17E-containing cells showed migration compared with wild-type cells (Fig. 2A). Furthermore, in the invasion assays, using a Matrigel®-coated chamber, invaded RhoA G17E cells were significantly higher than invaded wild-type cells (Fig. 2B). The number of RhoA Y42C cells that migrated and invaded were higher compared to the number of invading and migrating wild-type cells, but the increase was not significant. Epithelial mesenchymal transition (EMT) was considered to be the cause of

the increased motility of cells containing RhoA mutants. To confirm this hypothesis, we examined the mRNA expression of E-cadherin, Snail, Slug, Vimentin, and ZEB1, which are genes related to EMT. Real-time PCR showed that the expression of E-cadherin was significantly lower for G17E, but there was no difference in the expression levels of other genes (Fig. 2C).

The RhoA/Rho-associated protein kinase (ROCK) signaling pathway did not contribute to RhoA G17E-mediated cancer migration and invasion

We evaluated how the signals of the RhoA/ROCK-cofilin-actin pathway are regulated by RhoA mutations. As expected, transfer of RhoA G17E and RhoA Y42C induced the expression of ROCK and phosphorylated cofilin proteins (Fig. 3A); a ROCK inhibitor, Y-27632, suppressed the G17E-induced phosphorylation of cofilin in a concentration-dependent manner (Fig. 3B). To confirm that phosphorylated cofilin (inactive form) was involved in the G17E-mediated migration and invasion, migration and invasion assays using a transwell system were performed after the administration of Y-27632. Unexpectedly, cell migration was promoted by Y-27632 (Fig. 3C). Cell invasion was promoted for RhoA wild-type cells but remained unchanged for RhoA G17E-containing cells (Fig. 3D). We speculated that pathways other than the ROCK/cofilin pathway are involved in RhoA G17E-mediated cell migration and invasion.

RhoA G17E induced Vav1 expression and contributed to cancer invasion

To investigate the mechanism of RhoA G17E-mediated cancer invasion, we focused on Vav1, based on a previous report on angioimmunoblastic T-cell lymphoma [12]. Real-time PCR revealed that Vav1 mRNA expression was significantly increased in RhoA G17E-containing cells (Fig. 4A), and western blotting showed a significant elevation of Vav1 in cells with RhoA G17E and RhoA Y42C (Fig. 4B). We hypothesized that RhoA G17E regulated cancer cell migration and invasion through Vav1; to examine this, we performed Vav1 RNA interference. Vav1 was retrovirally knocked down by an shRNA in MKN74 cells; the efficiency of knockdown was confirmed by real-time PCR (Fig. 4C) and western blotting (Fig. 4D). The increase in G17E-containing migrating cells was reduced by Vav1 knockdown but not significantly (Fig. 4E). In contrast, the increase in infiltrating cells containing RhoA G17E was significantly reduced by Vav1 knockdown (Fig. 4F).

RhoA G17E and active Vav1 interacted through direct binding in MKN74 cells

To confirm the interaction of RhoA G17E and Vav1, we introduced RhoA G17E, containing an N-terminal FLAG tag, into MKN74 cells and performed a pull-down assay. RhoA with an N-terminal FLAG tag was immunoprecipitated with an anti-FLAG antibody conjugated to agarose beads, after which phosphorylated Vav1 expression was detected by western blotting. Phosphorylated Vav1 was specifically immunoprecipitated with RhoA G17E but not with RhoA WT (Fig. 5A).

The RhoA G17E-Vav1 signaling pathway induced cancer invasion via MMP-9

Next, we investigated how RhoA G17E-mediated induction of Vav1 expression affects downstream effector molecules. The expression of ROCK and phosphorylated cofilin, which are regulatory molecules

in the RhoA-ROCK pathway, were not changed, as observed by western blotting, even after Vav1 knockdown (Fig. 5B). As RhoAG17E/Vav1 signaling was found to regulate cancer cell invasion rather than migration, we focused on MMPs, which are known to degrade the extracellular matrix to regulate cancer invasion. According to gelatin zymography, MMP-9 expression was elevated by RhoA G17E transduction; this effect was abolished by knockdown of Vav1. In contrast, MMP-2 showed no change in expression upon RhoA G17E transduction (Fig. 5C). We further investigated the expression of SEK, JNK, and p38MAPK proteins, which are downstream regulators of Vav1. Unexpectedly, the expression of each of these proteins was reduced in RhoA G17E-containing cells compared to that in WT cells; knockdown of Vav1 did not affect this reduction (Fig. 5D). Unfortunately, we were unable to identify the key molecules regulating the RhoA G17E-Vav1 signal associated with MMP-9.

The RhoA G17E-Vav1 signal promoted peritoneal dissemination in vivo

Our results showed that the RhoA G17E-Vav1 signal enhanced the invasion and proliferation of the MKN74 cancer cells. Thus, we investigated how the RhoA G17E-Vav1 signal is involved in peritoneal dissemination in vivo, as it is known that this process occurs in diffuse gastric cancer. At 4 weeks after intraperitoneally injecting MKN74 cancer cells containing wild-type PhoA and RhoA mutants into nude mice, the number of intraperitoneal nodules was found to be significantly higher in mice injected with RhoA G17E-transduced cells than in mice injected with wild-type cells (Fig. 6A). Following intraperitoneal injection of RhoA G17E-transduced cells with Vav1 knockdown into nude mice, the number of peritoneal nodules in mice with RhoA G17E-transduced cells with Vav1 knockdown was greatly reduced compared to that in mice without Vav1 knockdown (scramble shRNA) (Fig. 6B). Hematoxylin and eosin (HE) staining of excised peritoneal disseminated nodules showed more invasive findings for G17E-containing cells compared to those for wild-type RhoA-containing cells (Fig. 6C).

Discussion

Diffuse gastric cancer is common in young women, tends to metastasize to the peritoneum, and has a poor prognosis. Although the clinical features of this cancer clearly differ from those of other gastric cancers, the treatment strategies for diffuse gastric cancer are similar. Here, we focused on RhoA mutations in diffuse gastric cancer, because a series of studies revealed a high frequency of RhoA mutations in this cancer [5-7]. In in vitro assays, overexpression of RhoA commonly promotes the proliferation and motility of cancer cells [10, 18 19] and is associated with poor prognosis [20]. In contrast, recent studies have shown that the inactivation of RhoA promoted colorectal cancer [21]. RhoA can promote or suppress the malignant phenotype depending on the cells and conditions. In a previous study [9], we introduced the most frequent RhoA mutants in gastric cancer, R5W, G17E, and Y42C, into a retrovirus vector. Distinct morphological changes were observed in MKN74 cells transduced with RhoA G17E and RhoA Y42C. Particularly, a spindle shape and sharp edges were obviously observed in cells containing RhoA G17E and to a lesser extent in cells containing RhoA Y42C. Our in vitro experiments showed that the RhoA mutants did not alter cell proliferation, but RhoA G17E promoted cancer cell migration and invasion in vitro. We initially hypothesized that the G17E-mediated morphological changes

and enhancement of migration and invasion may have been due to epithelial mesenchymal transition, although epithelial mesenchymal transition markers, such as snail and slug, showed no changes in expression. RhoA G17E mutations are rare in gastric cancer, accounting for only 3% of cases, but with the spread of genetic mutation profiling tests, the number of gastric cancer patients in whom G17E mutations are found is expected to increase. We have shown that RhoA G17E promotes gastric cancer cell migration and invasion via VAV1 and MMP9. Since VAV1 is strongly implicated in cancer prognosis and is a promising therapeutic target, we believe that further studies on RhoA mutations and VAV1 function are warranted.

We further examined signal changes in the RhoA-ROCK pathway mediated by RhoA mutations. The expression of phosphorylated cofilin, a downstream regulator of the RhoA-ROCK pathway, was increased by transduction of the RhoA G17E mutant. However, unexpectedly, the ROCK inhibitor did not suppress but rather enhanced RhoA G17E mutant-mediated migration and invasion of gastric cancer cells. This indicates that the RhoA-ROCK signaling pathway was not involved in G17E mutant-mediated cancer migration and invasion and other molecules and pathways may regulate migration and invasion.

Patients with angioimmunoblastic T-cell lymphoma, a subtype of T-cell lymphoma, frequently show RhoA mutations, mainly the G17 mutation, and it was recently reported that the RhoA G17 mutant is associated with Vav1 in this disease [12, 22, 23]. Vav1 is a member of the Rho guanine nucleotide exchange factor family and is specifically expressed in hematopoietic cells [24]. High expression of Vav1 is associated with a poor prognosis in various carcinomas, including gastric cancer. In pancreatic and lung cancer, cell proliferation is promoted by Vav1 [14, 15], and Vav1 promotes cell migration and matrix degradation through Rac and Cdc42 signaling in pancreatic cancer [14]. However, in breast cancer, Vav1 was reported to suppress Akt and negatively regulate the malignant phenotype [25]. Thus, like RhoA, Vav1 may function as a double-edged sword, supporting tumorigenesis and tumor progression, depending on the tumor type and condition [26]. In this study, although the expression of Vav1 in MKN74 cells could not be detected under normal culture conditions, the expression of both RhoA mRNA and protein became detectable only after transduction of RhoA G17E and Y42C. We hypothesized that the RhoA G17E mutant-mediated enhancement of MKN74 cell invasion and migration was mediated by Vav1. As expected, the enhanced MKN74 cell invasion mediated by the RhoA G17E mutant was obviously suppressed by Vav1 knockdown. In contrast, the knockdown of Vav1 did not significantly suppress G17E mutant-enhanced MKN74 cell migration. Only MKN74 cell invasion induced by the RhoA G17E mutant was demonstrated to be Vav1-mediated; Vav1-mediation of RhoA G17E mutant-induced migration could not be demonstrated. We further investigated the mechanism of RhoA G17E/Vav1-mediated cancer invasion. Expression of MKK4/SEK, p38MAPK, and JNK proteins, which are downstream effector molecules of Vav1, showed lower expression in cells with RhoA G17E than in wild-type cells (Fig. 5). We could not identify the effector molecules of Vav1 for RhoA G17E/Vav1-mediated cancer invasion in MKN74 cells, but MMPs, which are considered as the main factors affecting the invasion of cancer cells, were examined. Vav1 enhanced MKN74 cell invasion via MMP-9 but not via MMP-2. The details of the pathway connecting MMP-9 to Vav1 require further analysis.

In the xenograft model of peritoneal dissemination, the RhoA G17E mutant promoted peritoneal dissemination, and tumor formation was remarkably suppressed by knockdown of VAV1. This result indicates that RhoA G17E and Vav1 can be used as therapeutic targets for diffuse gastric cancer. Finally, upon examination of clinical specimens of gastric cancer, Vav1 expression was found to be significantly higher in diffuse gastric cancer and was found to be a poor prognostic factor. We did not measure the expression levels of the RhoA mutants in gastric cancer, which is a major limitation of this study. However, our results strongly suggest that the RhoA G17E mutant, Vav1, and related molecules can function as therapeutic targets for diffuse gastric cancer.

Conclusion

The RhoA G17E mutant induced Vav1 and enhanced cancer invasion via MMP-9 in gastric cancer cells. RhoA G17E/Vav1 promotes peritoneal dissemination and may be a useful therapeutic target for diffuse gastric cancer.

Abbreviations

RhoA: Ras homolog family member A, Vav1: vav guanine nucleotide exchange factor 1, CDH1: cadherin 1, Db1: DNA-binding oligopeptide, MMP-9: matrix metalloproteinase-9, RPMI: Roswell Park Memorial Institute, MAPK: mitogen-activated protein kinase, EGFR: epidermal growth factor receptor, FGFR2: fibroblast growth factor receptor 2, HER2: human epidermal growth factor receptor 2, KRAS: v-Ki-ras2 Kirsten rat sarcoma viral oncogene homolog, NRAS: Neuroblastoma RAS viral oncogene homolog, BRAF: B-Raf proto-oncogene, serine/threonine kinase, ROCK1: Rho associated coiled-coil containing protein kinase 1, SEK: SAPK/Erk kinase, MKK4: mitogen-activated protein kinase kinase 4, MAPK: mitogen-activated protein kinase, IgG: immunoglobulin G, HRP: horseradish peroxidase, DNA: deoxyribonucleic acid, PCR: polymerase chain reaction, cDNA: complementary dna, GAPDH: glyceraldehyde-3-phosphate dehydrogenase, mRNA: messenger ribonucleic acid, ZEB1: zinc finger E-box binding homeobox 1, RIPA: Radioimmunoprecipitation, BCA: Bicinchoninic acid, SDS-PAGE: Sodium dodecyl sulfate-Polyacrylamide gel electrophoresis, shRNA: short hairpin RNA, siRNA: small interfering RNA, NP-40: Nonidet P-40, FITC: fluorescein isothiocyanate, CCK-8: Cell Counting Kit-8, EMT: Epithelial mesenchymal transition, WT: wild type, MMP: matrix metalloproteinase, JNK: Jun amino terminal kinase, Rac: Ras-related C3 botulinum toxin substrate, Cdc42: cell division cycle 42

Declarations

Availability of data and materials

The following primer was used for confirming vector construction: 5’ATCTTGGTTCATTCTCAAGCCTC3’. A summary of inserted DNA sequencing data can be found in the Additional file 1. All-DNA seq data from this study are available for download through the NCBI Sequence Read Archive (SRA) (https://www.ncbi.nlm.nih.gov/sra/PRJNA726632), under accession number PRJNA726632.

Ethics approval and consent to participate

All animal experiments were carried out following the national standard of the care and use of laboratory animals, and the study was approved by the Animal Research Committee of Shinshu University (Matsumoto, Japan; approval no. 290088). The study was carried out in compliance with the ARRIVE guidelines.

Consent for publication

Not applicable

Availability of data and materials

The datasets used and/or analyzed in the current study are available from the corresponding author on reasonable request.

Competing interests

The authors declare that they have no competing interests.

Funding

No funding was received for this study.

Authors' contributions

SN, MKi, YS, MKo, TM, MT and YM contributed to the design of the study and editing of the manuscript. SN and MKi performed the experiments, contributed to data analysis, and wrote the manuscript. MKi and YS contributed to critical revision of the manuscript. SM, FM, ST, YY, TE, NH, MKuro, and HT participated in the experimental design and interpreted the acquired data. All authors read and approved the final manuscript.

Acknowledgements

Not applicable.

References

1. Global Burden of Disease Cancer C, Fitzmaurice C, Allen C, Barber RM, Barregard L, Bhutta ZA, Brenner H, Dicker DJ, Chimed-Orchir O, Dandona R *et al*: Global, Regional, and National Cancer Incidence, Mortality, Years of Life Lost, Years Lived With Disability, and Disability-Adjusted Life-years for 32 Cancer Groups, 1990 to 2015: A Systematic Analysis for the Global Burden of Disease Study. *JAMA Oncol* 2017, 3(4):524-548.

2. Bray F, Ferlay J, Soerjomataram I, Siegel RL, Torre LA, Jemal A: Global cancer statistics 2018: GLOBOCAN estimates of incidence and mortality worldwide for 36 cancers in 185 countries. *CA Cancer J Clin* 2018, 68(6):394-424.
3. Lauren P: The Two Histological Main Types of Gastric Carcinoma: Diffuse and So-Called Intestinal-Type Carcinoma. An Attempt at a Histo-Clinical Classification. *Acta Pathol Microbiol Scand* 1965, 64:31-49.
4. Stiekema J, Cats A, Kuijpers A, van Coevorden F, Boot H, Jansen EP, Verheij M, Balague Ponz O, Hauptmann M, van Sandick JW: Surgical treatment results of intestinal and diffuse type gastric cancer. Implications for a differentiated therapeutic approach? *Eur J Surg Oncol* 2013, 39(7):686-693.
5. Melo S, Figueiredo J, Fernandes MS, Goncalves M, Morais-de-Sa E, Sanches JM, Seruca R: Predicting the Functional Impact of CDH1 Missense Mutations in Hereditary Diffuse Gastric Cancer. *Int J Mol Sci* 2017, 18(12).
6. Kakiuchi M, Nishizawa T, Ueda H, Gotoh K, Tanaka A, Hayashi A, Yamamoto S, Tatsuno K, Katoh H, Watanabe Y *et al*: Recurrent gain-of-function mutations of RHOA in diffuse-type gastric carcinoma. *Nat Genet* 2014, 46(6):583-587.
7. Wang K, Yuen ST, Xu J, Lee SP, Yan HH, Shi ST, Siu HC, Deng S, Chu KM, Law S *et al*: Whole-genome sequencing and comprehensive molecular profiling identify new driver mutations in gastric cancer. *Nat Genet* 2014, 46(6):573-582.
8. Cancer Genome Atlas Research N: Comprehensive molecular characterization of gastric adenocarcinoma. *Nature* 2014, 513(7517):202-209.
9. Etienne-Manneville S, Hall A: Rho GTPases in cell biology. *Nature* 2002, 420(6916):629-635.
10. Chang KK, Cho SJ, Yoon C, Lee JH, Park DJ, Yoon SS: Increased RhoA Activity Predicts Worse Overall Survival in Patients Undergoing Surgical Resection for Lauren Diffuse-Type Gastric Adenocarcinoma. *Ann Surg Oncol* 2016.
11. Zheng Y: Dbl family guanine nucleotide exchange factors. *Trends Biochem Sci* 2001, 26(12):724-732.
12. Fujisawa M, Sakata-Yanagimoto M, Nishizawa S, Komori D, Gershon P, Kiryu M, Tanzima S, Fukumoto K, Enami T, Muratani M *et al*: Activation of RHOA-VAV1 signaling in angioimmunoblastic T-cell lymphoma. *Leukemia* 2018, 32(3):694-702.
13. Fernandez-Zapico ME, Gonzalez-Paz NC, Weiss E, Savoy DN, Molina JR, Fonseca R, Smyrk TC, Chari ST, Urrutia R, Billadeau DD: Ectopic expression of VAV1 reveals an unexpected role in pancreatic cancer tumorigenesis. *Cancer Cell* 2005, 7(1):39-49.
14. Sebban S, Farago M, Rabinovich S, Lazer G, Idelchuck Y, Ilan L, Pikarsky E, Katzav S: Vav1 promotes lung cancer growth by instigating tumor-microenvironment cross-talk via growth factor secretion. *Oncotarget* 2014, 5(19):9214-9226.
15. Razidlo GL, Magnine C, Sletten AC, Hurley RM, Almada LL, Fernandez-Zapico ME, Ji B, McNiven MA: Targeting Pancreatic Cancer Metastasis by Inhibition of Vav1, a Driver of Tumor Cell Invasion.

Cancer Res 2015, 75(14):2907-2915.

16. Kang L, Hao X, Tang Y, Zhao Z, Zhang H, Gong Y: Elevated level of Vav1 was correlated with advanced biological behavior and poor prognosis in patients with gastric cancer. *Int J Clin Exp Pathol* 2018, 11(1):391-398.
17. Livak KJ, Schmittgen TD: Analysis of relative gene expression data using real-time quantitative PCR and the 2(-Delta Delta C(T)) Method. *Methods* 2001, 25(4):402-408.
18. Nishizawa T, Nakano K, Harada A, Kakiuchi M, Funahashi SI, Suzuki M, Ishikawa S, Aburatani H: DGC-specific RHOA mutations maintained cancer cell survival and promoted cell migration via ROCK inactivation. *Oncotarget* 2018, 9(33):23198-23207.
19. Liu J, Li S, Chen S, Chen S, Geng Q, Xu D: c-Met-dependent phosphorylation of RhoA plays a key role in gastric cancer tumorigenesis. *J Pathol* 2019, 249(1):126-136.
20. Ushiku T, Ishikawa S, Kakiuchi M, Tanaka A, Katoh H, Aburatani H, Lauwers GY, Fukayama M: RHOA mutation in diffuse-type gastric cancer: a comparative clinicopathology analysis of 87 cases. *Gastric Cancer* 2016, 19(2):403-411.
21. Rodrigues P, Macaya I, Bazzocco S, Mazzolini R, Andretta E, Dopeso H, Mateo-Lozano S, Bilic J, Carton-Garcia F, Nieto R *et al*: RHOA inactivation enhances Wnt signalling and promotes colorectal cancer. *Nat Commun* 2014, 5:5458.
22. Sakata-Yanagimoto M, Enami T, Yoshida K, Shiraishi Y, Ishii R, Miyake Y, Muto H, Tsuyama N, Sato-Otsubo A, Okuno Y *et al*: Somatic RHOA mutation in angioimmunoblastic T cell lymphoma. *Nat Genet* 2014, 46(2):171-175.
23. Boddicker RL, Razidlo GL, Feldman AL: Genetic alterations affecting GTPases and T-cell receptor signaling in peripheral T-cell lymphomas. *Small GTPases* 2019, 10(1):33-39.
24. Bonnefoy-Berard N, Munshi A, Yron I, Wu S, Collins TL, Deckert M, Shalom-Barak T, Giampa L, Herbert E, Hernandez J *et al*: Vav: function and regulation in hematopoietic cell signaling. *Stem Cells* 1996, 14(3):250-268.
25. Grassilli S, Brugnoli F, Lattanzio R, Marchisio M, Perracchio L, Piantelli M, Bavelloni A, Capitani S, Bertagnolo V: Vav1 downmodulates Akt in different breast cancer subtypes: a new promising chance to improve breast cancer outcome. *Mol Oncol* 2018.
26. Zandvakili I, Lin Y, Morris JC, Zheng Y: Rho GTPases: Anti- or pro-neoplastic targets? *Oncogene* 2017, 36(23):3213-3222.

Figures

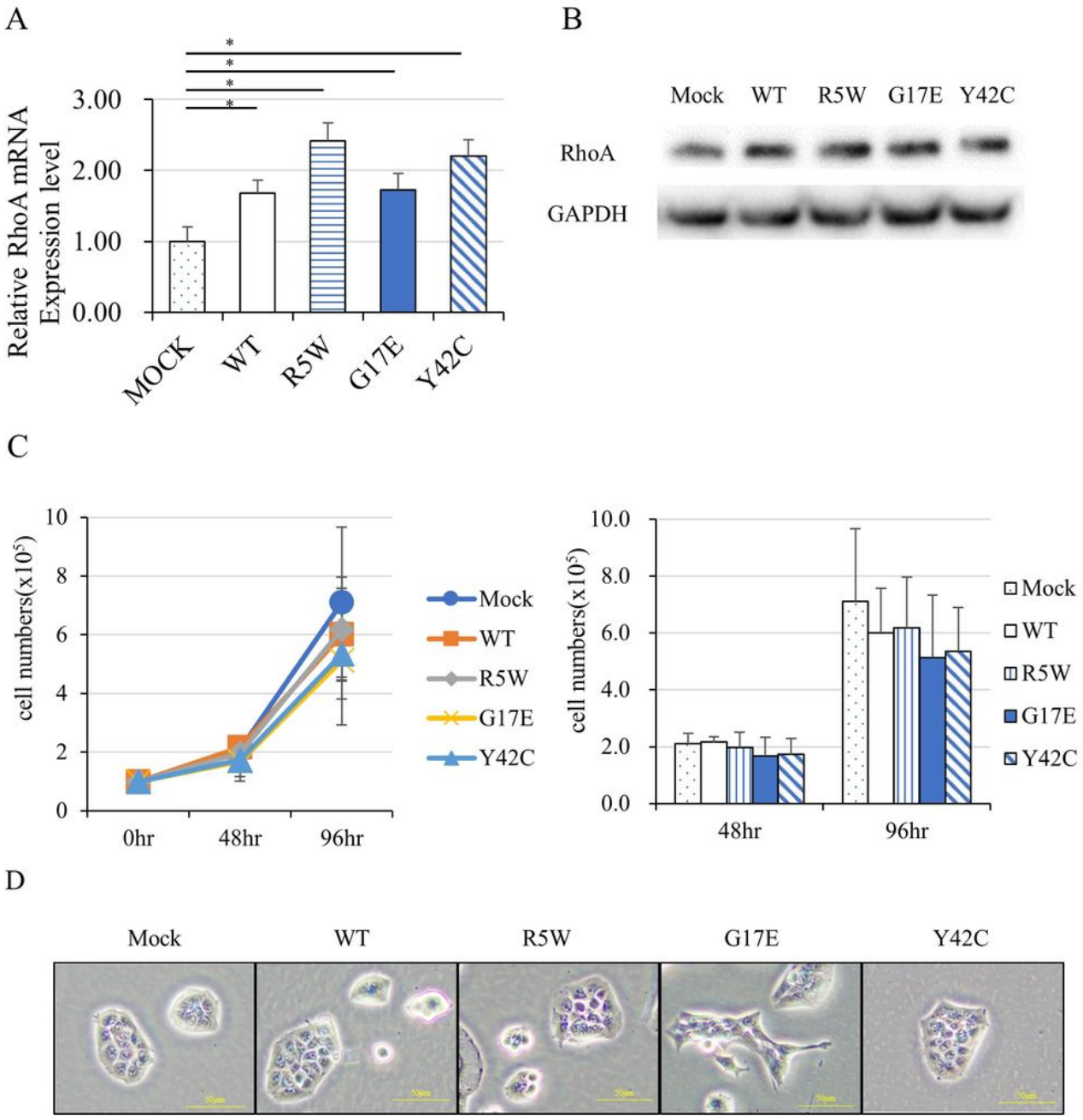

Figure 1

RhoA mutations induced morphological changes in MKN74 cells. (a) RhoA mRNA expression of MKN74 cells transduced with RhoA wild type or RhoA mutants, RhoA R5W, G17E, and Y42C, as determined by real-time PCR (N=5). (b) RhoA protein expression in MKN74 cells transduced with a vector containing RhoA mutants by western blot analysis. GAPDH was used as an internal control. (c) Morphological changes in MKN74 cells transduced with a vector containing RhoA mutants and (d) proliferation of these

cells after 96 h of culture (N=4). Results are presented as the mean ± standard deviation. Significance of differences was determined by Dunnett's test. *P < 0.05

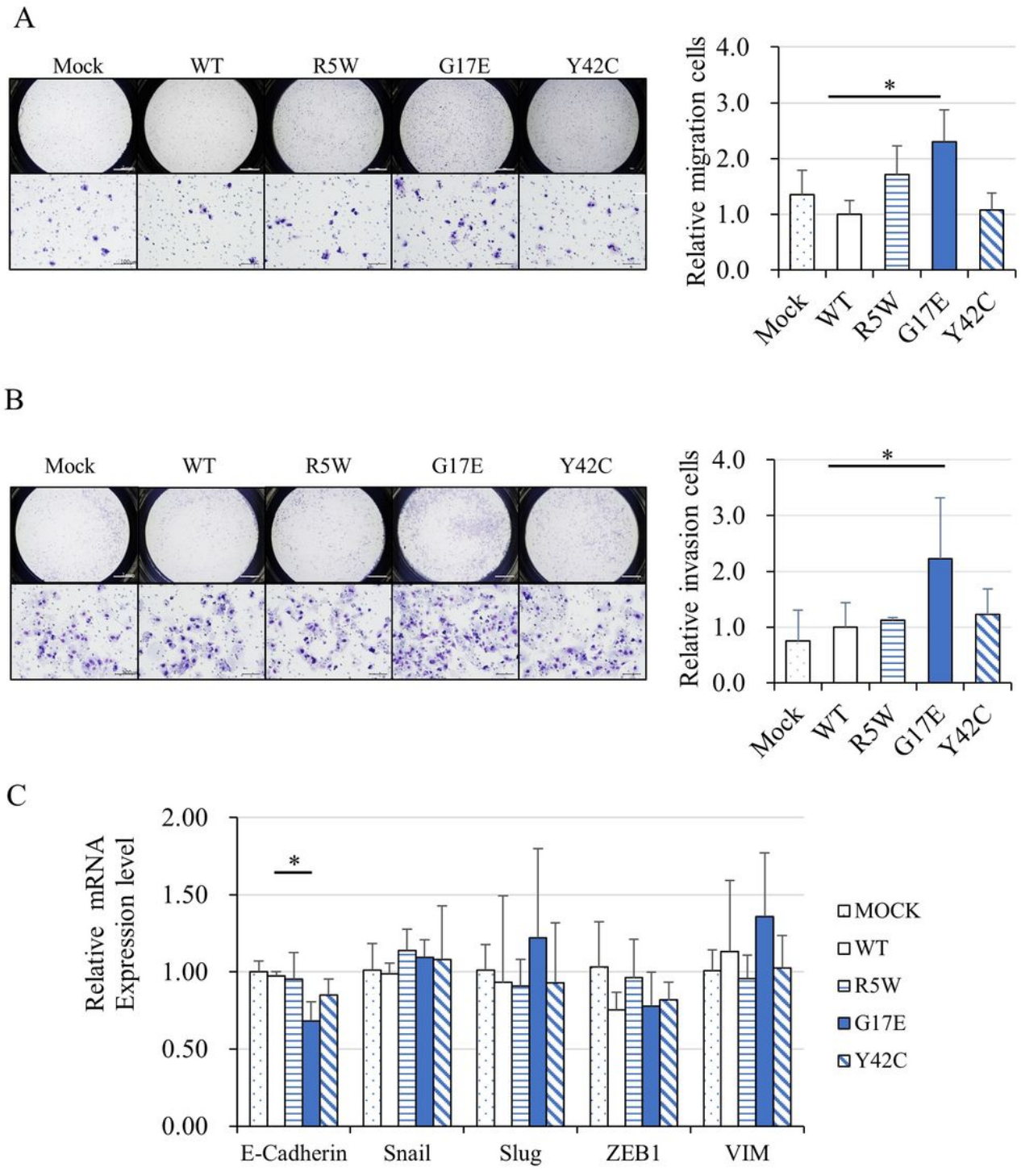

Figure 2

RhoA G17E mutation promoted migration and invasion of MKN74 cells. (a) Transwell assays showed that RhoA G17E significantly enhanced the migration of MKN74 cells (N=4). (b) Matrigel-coated transwell assays showed that RhoA G17E significantly promoted the invasion of MKN74 cells (N=4). (c) Real-time

PCR showed that the expression level of E-cadherin was significantly lower in cells containing the G17E mutant. (N=5) The results are presented as mean ± standard deviation, Significance of differences was determined by Dunnett's test. *P < 0.05

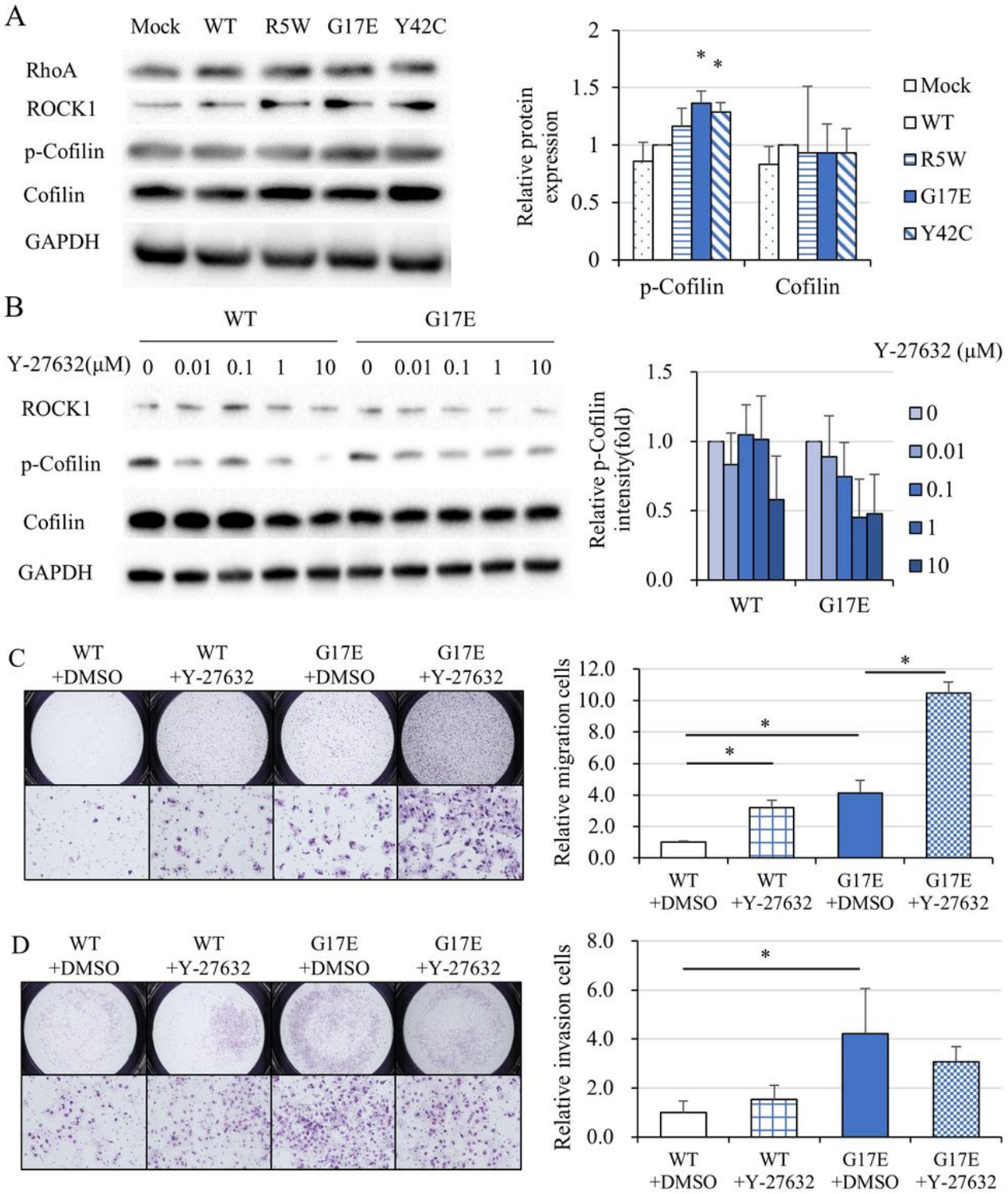

Figure 3

Introduction of RhoA mutations activated the ROCK signaling pathway, whereas inhibition of the ROCK signaling pathway unexpectedly enhanced cell motility. (a) Protein expression of the RhoA-ROCK

signaling pathway in MKN74 cells transduced with a vector containing RhoA mutants. Transduction of the RhoA G17E and Y42C mutant-containing vector enhanced the expression of ROCK and phosphorylated cofilin proteins. (b) The ROCK inhibitor, Y-27632, suppressed the RhoA G17E-induced phosphorylation of cofilin in a concentration-dependent manner. (c) Migration and invasion assays of MKN74 cells transduced with RhoA WT and the RhoA G17E mutant using a transwell system with 10 μM Y-27632 (N=4). Inhibition of the ROCK signaling pathway unexpectedly enhanced cell motility in both RhoA WT- and RhoA G17E-containing cells. (d) Invasion assays of MKN74 cells transduced with a RhoA WT- or RhoA G17E mutant-containing vector using a Matrigel-coated transwell system with 10 μM Y-27632 (N=4). Cell invasion was promoted significantly in cells with RhoA WT but was not significantly changed in cells with the RhoA G17E mutant. The results are presented as mean ± standard deviation. Significance of differences was determined by Student's t-test and Dunnett's test. *P < 0.05

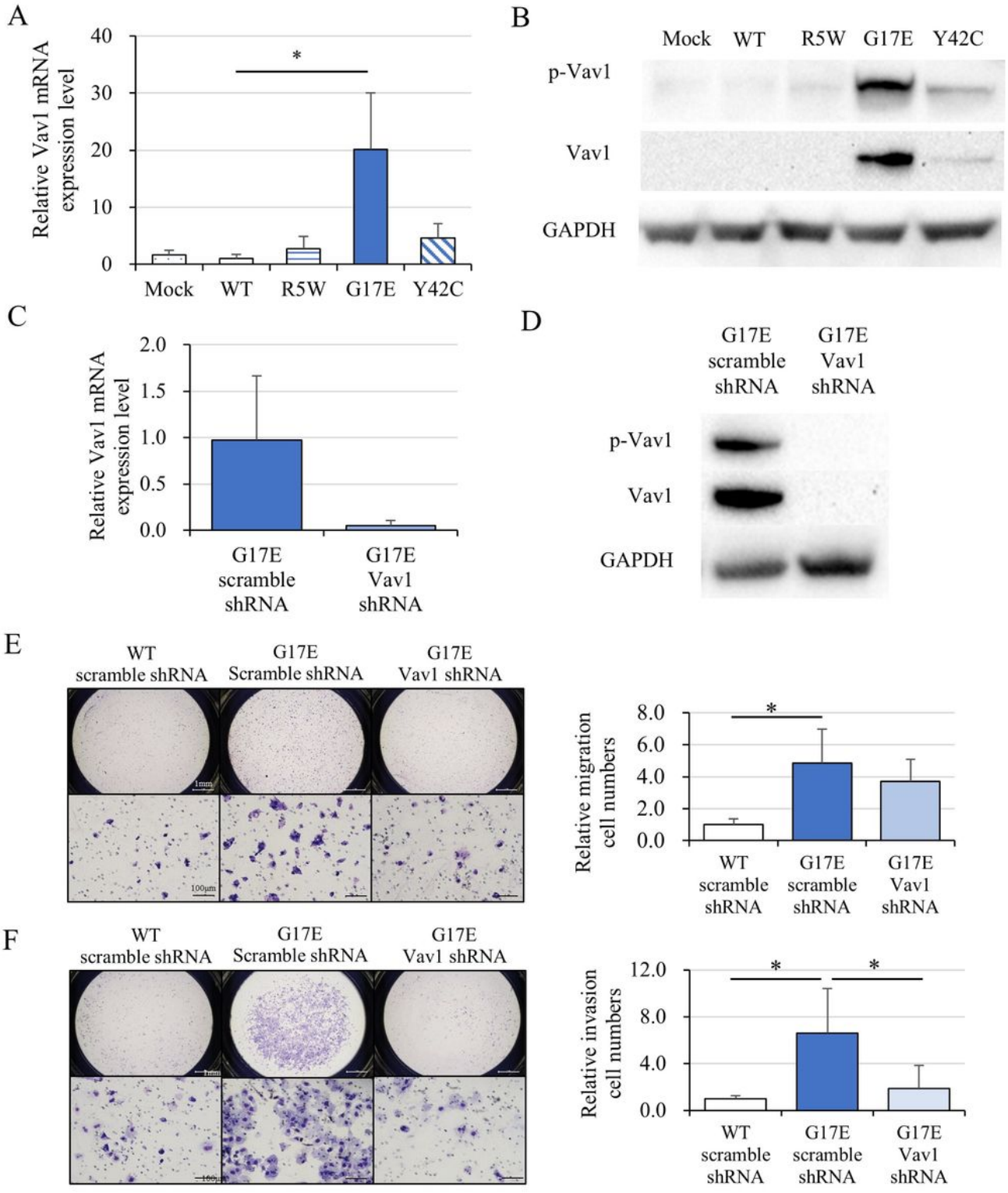

Figure 4

RhoA G17E induced Vav1 expression and contributed to the invasion of MKN74 cells. (a) Vav1 mRNA expression in MKN74 cells transduced with a vector containing a RhoA mutant (N=5). Real-time PCR revealed that Vav1 mRNA expression was significantly increased in cells with the RhoA G17E mutant. (b) Vav1 protein expression of MKN74 cells transduced with a vector containing mutant RhoA. GAPDH was used as an internal control. Western blotting showed significant elevation of Vav1 and phosphorylated

Vav1 in cells with RhoA G17E and Y42C mutants. (c, d) Vav1 was retrovirally knocked down by Vav1 shRNA, and its expression was compared with that in cells transfected with scramble shRNA in MKN74 cells transduced with the RhoA G17E mutant by real-time PCR and western blotting. (e) Migration assays of cells containing the RhoA G17E mutant with Vav1 shRNA and scrambled control shRNA (N = 4). The increased migration of cells with RhoA G17E was reduced by Vav1 knockdown but not significantly. (f) Invasion assays of MKN74 cells transduced with a vector containing the RhoA G17E mutant and treated with Vav1 shRNA and scrambled control shRNA (N=4). Increased infiltration of cells transduced with the RhoA G17E mutant was significantly reduced by Vav1 knockdown. The results are presented as mean ± standard deviation. Significance of differences was determined by Student's t-test and Dunnett's test. *P < 0.05

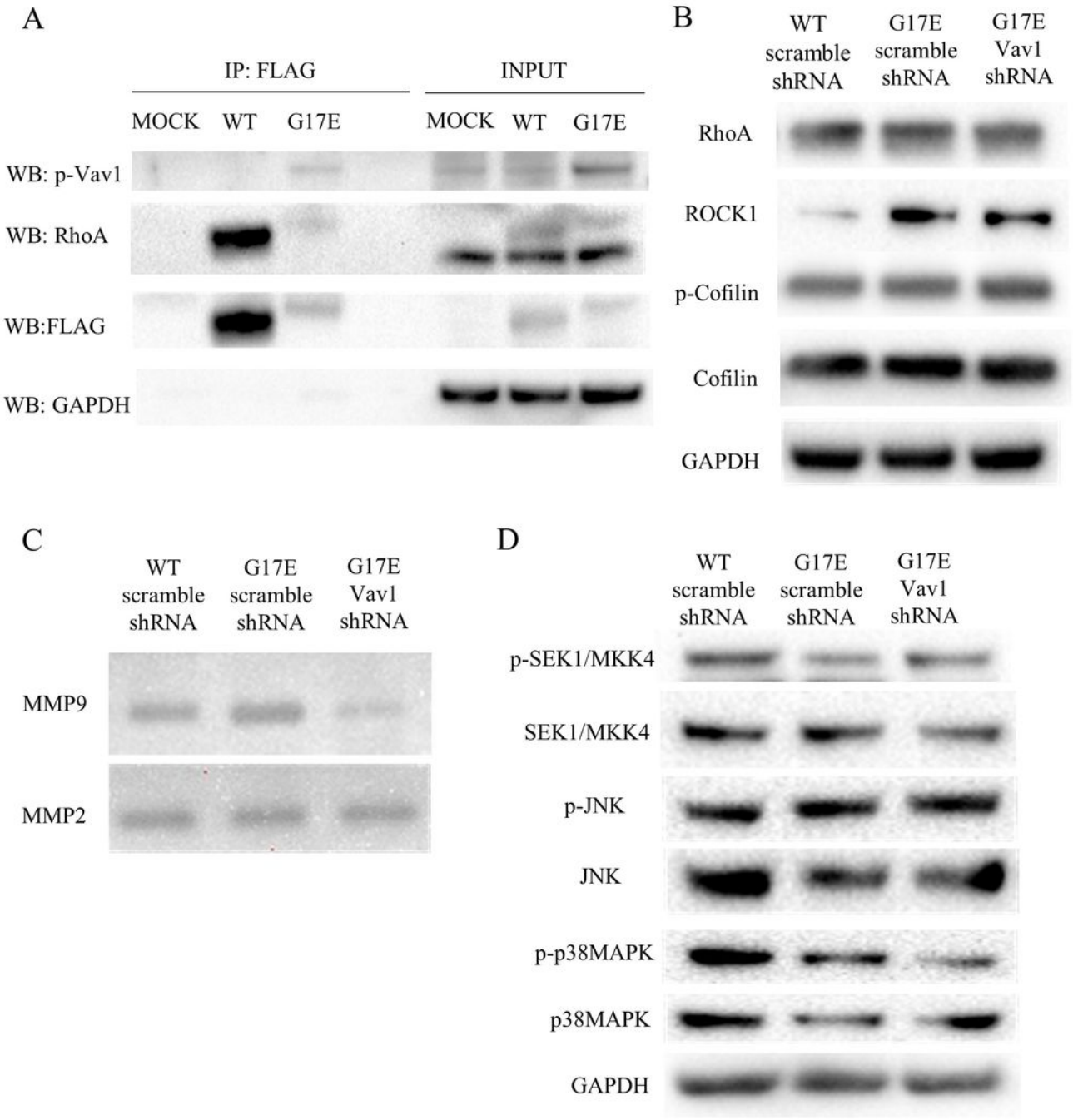

Figure 5

RhoA G17E and active Vav1 interacted through direct binding and induced cancer invasion via matrix metalloproteinase-9 (MMP-9). (a) Binding of Vav1 to RhoA G17E detected by immunoprecipitation. Phosphorylated Vav1 was specifically immunoprecipitated with RhoA G17E but not with RhoA WT. (b) Expression of proteins related to the RhoA-ROCK pathway after treatment with Vav1 shRNA. The expression of ROCK and phosphorylated cofilin was unchanged after Vav1 knockdown. (c) Enzymatic

activities of MMP-2 and MMP-9 examined by gelatin zymography. Expression of MMP-9 was elevated by RhoA G17E gene transduction; this effect was abolished by knockdown of Vav1. MMP-2 expression showed no change. (d) Expression of proteins related to the MAPK pathway, which is thought to be downstream of Vav1, after treatment with Vav1 shRNA, was reduced in RhoA G17E mutant-containing cells compared to that in WT RhoA-containing cells; this reduction was unaffected by knockdown of Vav1.

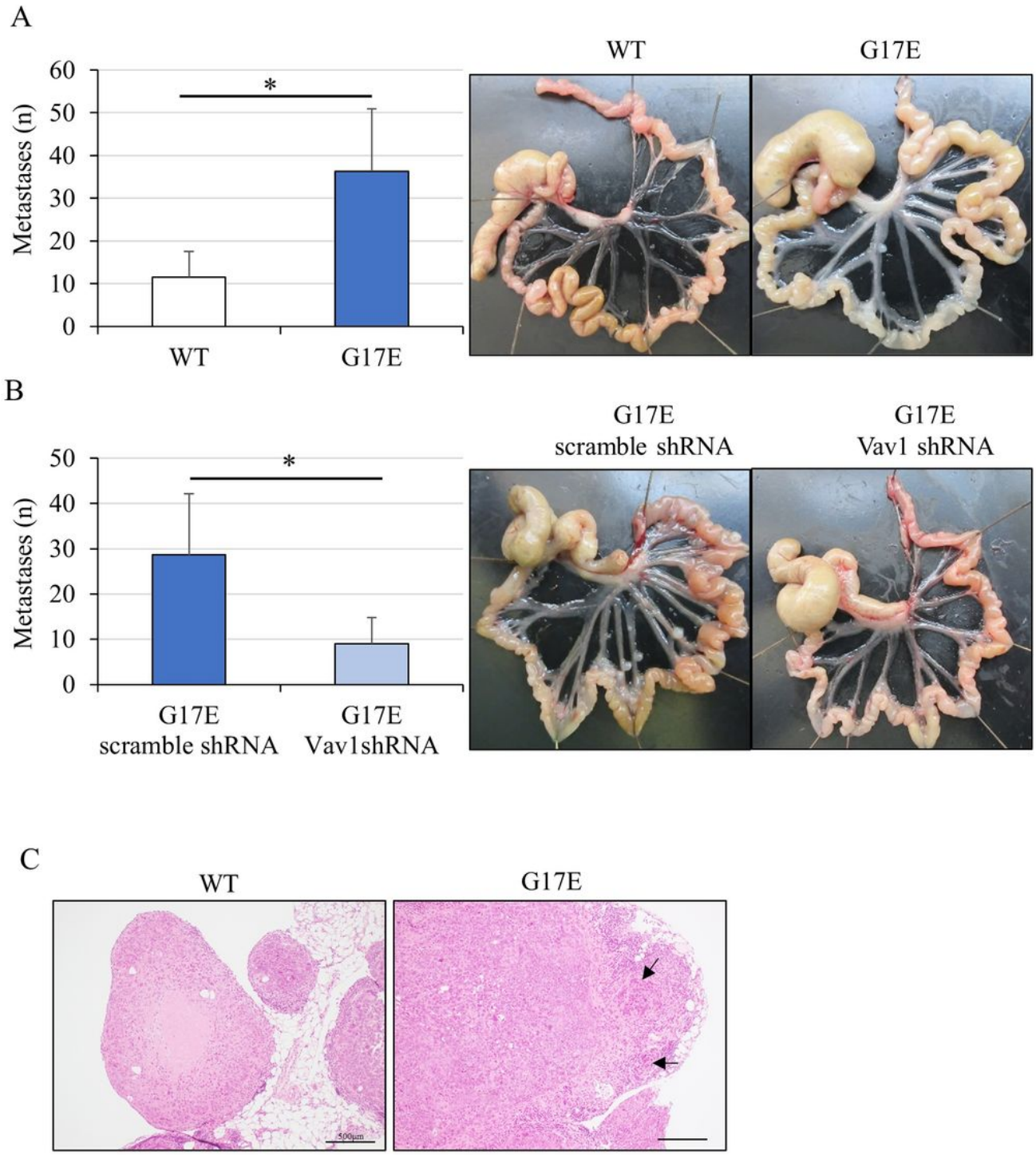

Figure 6

Vav1 promoted the formation of peritoneal disseminated nodules in vivo. (a) Number of peritoneal disseminated nodules after intraperitoneal administration of RhoA WT and RhoA G17E mutant. Arrow indicates a peritoneal disseminated nodule. The number of intraperitoneal nodules was significantly higher in mice injected with RhoA G17E-containing vector-transduced cells than in cells transduced with a vector containing WT RhoA. (b) Number of peritoneal disseminated nodules after intraperitoneal administration of RhoA G17E mutant-containing vector-transduced cells with Vav1 shRNA or scrambled control shRNA. The number of peritoneal nodules in RhoA G17E mutant-containing vector-transduced cells with Vav1 knockdown was greatly reduced compared to that in RhoA G17E mutant-containing vector-transduced cells without Vav1 knockdown (scramble shRNA). (c) HE staining of the excised peritoneal disseminated nodules showed infiltrative tumor growth of G17E mutant-containing cells. Arrows indicate infiltrated tumor cells. The results are presented as mean ± standard deviation. Significance of differences was determined by Student's t-test. *P < 0.05

Supplementary Files

This is a list of supplementary files associated with this preprint. Click to download.

- Additionalfile1..tif
- Additionalfile2..tif
- Additionalfile3..tif
- Additionalfile4..tif
- Additionalfile5..tif